

A Unified Optimal Design Approach for Geometrically Nonlinear Skeletal Dome Structures

Tugrul Talaslioglu^{1*}

¹ Department of Civil Engineering,
Osmaniye Korkut Ata University, 8000, Osmaniye/Turkey

* Corresponding author, e-mail: ttalaslioglu@osmaniye.edu.tr

Received: 19 October 2018, Accepted: 04 March 2019, Published online: 10 April 2019

Abstract

In this study, a unified optimal design approach is proposed for the design of skeletal dome structure (SDS). Thus, this study has three objectivities, i) presenting the emergence of proposed design integrity, ii) applying the proposed optimal design approach for the design optimization geometrically nonlinear SDS with both ellipse and sphere-shaped forms considering both the shape, size and topology-related design variables, iii) determining the dominant design criteria in the design of SDS. In this framework, the design of SDS is optimized thereby minimizing its entire weight and joint displacements and maximizing its member forces at the same time. The design constraints are borrowed from the provisions of American Petroleum Institute (API RP2A-LRFD) specification. A multi-objective optimization algorithm (MOA) named Pareto Archived Genetic Algorithm (PAGA), as an optimization tool is integrated by an automatic dome generating tool. Therefore, the novelty of this study comes from being the first attempt to obtain the optimal design in a way of integrating both member and joint-related design constraints by the geometrically nonlinear structural analysis. Consequently, it is displayed that that the proposed optimal design approach facilitates to determine an appropriate optimal design through a tradeoff analysis for designers depending on their preferences. The design concepts concerned with buckling, axial stress, combination of axial & bending, and yielding have the higher dominant effects in the optimal design of SDS. Furthermore, it is also demonstrated that the inclusion of diagonal members into the design of SDS provides a reduction in the violation of dominant design constraints.

Keywords

dome structure, geometric nonlinearity, multi-objective optimization, API RP2A-LRFD

1 Introduction

The dome structures as a member of skeletal structural systems have a reputation of spanning the large areas without requiring any interior support. Therefore, they have accomplished to take a part in almost every period of historical progression in the structural system. Particularly, SDS comes into prominence through the development in the steel industry. In this regard, the designers have been incessantly in hot pursuit of using a more realistic and rational design approach for the design of SDS. In general, the engineering judgment decided by the designers is carried out depending on both the satisfactory degree of basic design criteria and accumulated experiences of designers. However, this achievement-oriented approach based on theoretical expertise and practical experiences generally omits the consideration of other design factors such as the higher nodal displacements, global stability and etc. Therefore, the confidence level that indicates about the performing capacity

of SDS against any failure incident is relatively reduced. In order to deal with this assuring-related design problem, there exists fortunately a statistical-based analysis technique named reliability analysis [1]. Thus, it is possible to measure and estimate the probability of failure depending on a number of quantitative observations such as stresses, displacements of SDS members and joints. However, there also exists the qualitative type data such as the structural analysis which is utilized to compute the responses of SDS members [2–3]. It is easily seen that the quantitative and qualitative concepts are also interacted with each other's.

In fact, there exist two fundamental notions that manages the qualitative measurements along with the quantitative one: *incompleteness* and *uncertainty*. An appropriate arrangement in the design requirements according to these concepts allows the designer to obtain a design against the occurrence of any failure incident [1, 4].

One of the reasons behind incompleteness and uncertainty is arisen from the lack of information or knowledge about the modelling and analyzing issues in the design of SDS. Furthermore, it has to be noted that this lack has also responsibility of occurring the failure incident in the design of SDS. In this regard, the mechanism behind the failure incident has to be firstly introduced.

A well-known failure incident named "collapse" has a big importance in the design of SDS due to the higher probability of occurring during or after building the SDS [5]. There are several reasons of occurring the collapse-induced failure (CIF) in SDS such as local and/or global buckling of structural members and/or systems, design, construction-related errors and etc. [6]. The recent studies particularly focus on one type of CIF that starts with a localized damage and ends with a local or global structural failure [7–15]. In order deal with this type failure, the best reasonable design approach is to increase both the number and the cross-sectional size of structural members. However, it is obvious that the constructing cost is accordingly elevated. The other design complexity is concerned with the determination of appropriate modelling and analyzing approach since the joint displacements may be larger in SDS.

Although this study does not propose a probability or possibility-based assessment of failure incidents, several *weak links*, which play a big role in gathering the qualitative and quantitative data, are identified and highlighted in order to develop a new design methodology.

Thus, the following part is reserved to investigate the weak links in the design of SDS and accordingly highlight their effects on the design of SDS considering the incompleteness and uncertainty concepts.

Integration of a compact design specification

There exist a big variety in the member cross-sectional size and geometrical dimensions of SDS. This situation points out not only a higher probability of including a slender member into SDS but also an occurrence of local or global stability induced failure leading to the collapse of SDS. The other design factor that governs the mechanism of CIF is concerned with the excessive number of joints. Similarly, the higher variety in the connecting components (weld, bolt, rivet and etc.) and the connecting topology causes to increase the risk of CIF due to the probability of occurring a lower joint strength in SDS. The ductility capacity of joint and members also plays a big role in the management of CIF mechanism. Because, an increase in firstly joint displacements and then the member

deformations cause to begin a sudden plastic action. At this point, it has to be noted that a higher ductility capacity of SDS provides a big advantage for load-carrying capacity but a disadvantage for the serviceability capacity of SDS.

The plastic incident is generally occurred depending on an increase in the axial force in the horizontal members of SDS and resulted by a plastic hinge on the related members [16–18]. Although there exists a possibility of carrying the extra member responses through the longitudinal members, the extra rotations occurred in the plastic hinges may cause a stability failure in SDS. Therefore, the strength and ductility capacities of both member and joint have to be checked at the design stage according to the provisions of available design specification. Therefore, the use of a compact design code reduces the incompleteness degree encountered in a number of design codes.

Use of an appropriate structural analysis approach

Due to the discrete nature of SDS, there exists a high tendency to inherently a significant configurational change in its structural system under any external loading condition. Although the member responses of SDS are well below a yield point of material, the nodal displacements of SDS may suddenly reach to the higher values [19–21]. In fact, the larger nodal displacements cause also to be arisen a global stability-related failure in SDS although the stabilities of SDS members are not lost. Assuming the structural system of skeletal dome to exhibit a nonlinear behavior becomes to be more realistic. Therefore, the fundamentals of proposed structural analysis have to be constituted on the geometric nonlinearity. Furthermore, the proposed structural analysis approach has also a capability of solving the global stability problem. Tackling the global stability as a linear eigen-value problem is unfortunately not an appropriate solution due to obtaining the global stability capacity at the higher value [20]. In this regard, the equilibrium path, which shows the correlation between member response and nodal displacement, has to be traced by an incremental-iterative based structural analysis approach.

Unfortunately, this equilibrium path is represented by a nonlinear curve, which contains a number of critical points such as bifurcation, point, limit point and etc. In fact, this equilibrium path is also utilized to determine the global buckling capacity of SDS through monitoring the sudden change in the critical points. Therefore, the use of efficient nonlinear structural analysis approach reduces the uncertainty degree in the computation of both member responses and global stability capacity of SDS.

Providing a higher structural serviceability for SDS

It is mentioned that the serviceability capacity of SDS may be decreased due to the increase in the ductility capacity. In order to increase the serviceability capacity of SDS for an achievement of obtaining a motion-insensitive structural system, the best remedy is to bound the joint displacements by an upper limit [22]. A satisfied balance between the serviceability and ductility capacities of SDS correspondingly reduces the uncertainty degree.

Integration of an optimization tool

It is emphasized that the design complexity of SDS is higher with respect to the design of other structural systems. One of the reasons behind the design complexity generally arisen from simultaneously seeking a lower constructing cost for the economic efficiency, a higher load-carrying capacity for the safety purpose and a lower joint displacement for the higher serviceability. Furthermore, the variety in the cross-sectional size of SDS members and geometrical dimensions in SDS also increases the design complexity due to stimulatingly satisfying these objective functions at a higher level. Because, the use of lower cross-sectional size along with the decreased number of members makes an additional profit for the construction of SDS system but an additional risk for CIF incident in SDS. The most reasonable and realistic solution is to involve an optimization tool into the design stage of SDS. Particularly, the employed optimization tool has to be capable of handling with multiple objective functions [22–26]. Thus, it is possible to make a trade-off analysis in order to the most appropriate design according to the preference of designer. The use of multi-objective optimization approach reduces the incompleteness degree in a way of providing an opportunity of making a trade-off analysis for the designers.

Integration of an automatic dome generating tool for conceptual geometric configuration of SDS

Although the integration of multi-objective optimization tool provides a big contribution for the determination of appropriate design, a further convergence degree in the optimal design is obtained by arranging the geometrical configuration of SDS. Particularly, a consistent variety in the geometrical configuration of SDS leads to a positive contribution in the increase of load-carrying capacity thereby reducing the probability of the stability-related problem. Thus, the uncertainty degree arisen from using a pre-assumed conceptual configuration for SDS is accordingly decreased.

In the framework of these insightful descriptions, this study accomplishes to provide an intelligent computer based design integrity for SDS design. In this regard, the

design of SDS with various geometrical configurations is optimized thereby utilizing a MOA named Pareto Archived Genetic Algorithm (PAGA) along with the displacement, joint and member-related design constraints. It is noted that the computing performance of PAGA was also evaluated considering several multi-objective evolutionary algorithms named NSGAI [27], SMSEMOA [28], MOEA/D [29], PESAI [30], SPEA2 [31], eMOEA [32], [21].

The organization of this study begins with an introduction to the intelligent computer based optimal design methodology. Then, the sections 3 and 4 are reserved for the discussion of results and conclusion.

2 An intelligent computer based optimal design methodology

This study proposes an intelligent computer based design integrity in order to optimize the design of SDS. In fact, its working mechanism is emerged considering the design-related lacks which come from the weak-links mentioned in preceding chapter. Thus, this section is separated into two sub-sections: a brief introduction to the optimization tool PAGA and description its governing elements of proposed intelligent computer-based optimal design methodology.

2.1 A brief introduction to PAGA

The proposed optimal design approach utilizes an evolutionary based multi-objective optimization tool named PAGA. In fact, the evolutionary-based methodologies have been widely used in the optimization of structural engineering design problems [22–32]. Particularly, SDS achieves to become one of attractive application areas in the evolutionary-based design optimization field [33–44].

The evolutionary-based search mechanism of PAGA is managed by the four sub-populations utilized to represent the entire solution space by four sub-solution regions (see Fig. 1). These sub-populations have the responsibility of both exploring and exploiting the promising genetic material. Particularly, the size of sub-population and the values of genetic operator parameters are utilized for the exploitation of genetic material.

The execution of PAGA starts by assigning the genetic-related parameter values (see Fig. 2). Then, the fitness values of current population is computed. The pareto solutions are determined and stored in a separate pareto-archived population. Because, the basic statistical data obtained from pareto-archived population is used to adjust the sub-population sizes depending on a parameter named "division number" that is pre-assumed and utilized to for

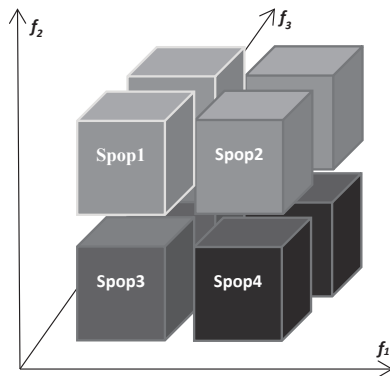


Fig. 1 Visualization of Sub-populations Utilized by PAGA

```

Define the objective functions  $f_1, f_2, f_3$  along with the upper and lower values of design variables
Initialize the genetic parameter values named generation number, population size, sub-generation number1, sub-
generation number2 and a division number
for i=1: generation number
    Compute fitness values and determine current pareto solutions
    Compute the statistical data regarded with the current pareto solutions
    Compute sub-population size1, sub-population size2, sub-population size3 and sub-population size4
    Compute the values of Genetic Parameters
    Evaluate sub-population1, sub-population2, sub-population3 and sub-population4
    Correct sub-population1, sub-population2, sub-population3 and sub-population4 according to the upper and lower
    values of design variables
end
    
```

Fig. 2 A Pseudo Code for the Description of Working Mechanism of PAGA

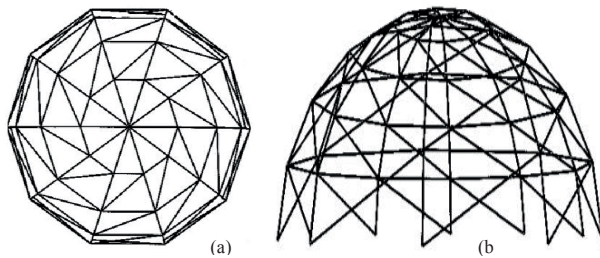


Fig. 3 Top (a) and Side (b) View of SDS Used as a Conceptual Model

the determination of promising solution regions. Furthermore, the genetic operator parameter values are also adjusted depending on the pre-assumed sub-generation numbers and generation number. In this regard, two basic genetic operators named simulated binary crossover and polynomial mutation manages the combination and diversification of genetic material embedded in the individuals of population. If it is required, the individuals of generated population are re-computed according to the upper and lower values of design variables. Following the computation of fitness values of current population individuals and determination of pareto solutions, the evolutionary search of PAGA continues until the pre-assumed generation number is completed. The further details about the working mechanism of PAGA is presented in [21].

The search capacity of PAGA for an optimal design with higher convergence degree is increased through inclusion of automatic dome generating tool into the proposed optimal design procedure. Thus, only certain dimensions

of SDS, for example their spanning distances and heights become to be adequate in the generation of various SDS with different topological, size and shapes (see a conceptual SDS in Fig. 3). The design constraints are based on the provisions of API RP2A-LRFD specification which is the most comprehensive one of compact design codes. The serviceability capability of SDS is kept under the control thereby limiting the joint displacements by an upper bound. The member responses under the external static loads are computed by a trend nonlinear structural analysis approach named "arc length" which is proved to be successful in both tracing the equilibrium path and identifying the critical points located on the equilibrium path [20–22]. Thus, it is possible to compute the global stability capacity of SDS by the arc length method while the member stability capacity is checked through the use of the provisions of API RP2A-LRFD specification. The proposed optimal design procedure is coded in MATLAB software in a way integrating ANSYS software which has a responsibility of computing the member responses.

At this point, the novelty of this study comes from being the first attempt about integrating the available design code with the nonlinear structural analysis approach. The other important feature of proposed optimal design approach is its higher flexibility of easily involving any available design code into its design procedure

2.2 The basic issues governing the proposed intelligent computer based optimal design methodology

The proposed design optimization of the dome structures simultaneously minimizes the entire weight of SDS and nodal displacements and maximizes the member forces at the same time. The proposed optimal design approach in associated with a penalizing procedure, elements of which are based on provisions of API RP2A-LRFD specification is formulated as:

$$f_1 = \min \left(\sum_{k=1}^m (w \cdot l)_k + P_1 \right), \quad (1)$$

$$f_2 = \min(d_{ij} + P_2) \quad (i = 1, \dots, 12 \text{ and } j = 1, \dots, n), \quad (2)$$

$$f_3 = \max(f_{ij} + P_3) \quad (i = 1, \dots, 12 \text{ and } j = 1, \dots, n). \quad (3)$$

The entire weight of dome structure, member forces and nodal displacements are represented by f_1 (m , number of dome member; w , unit weigh per member length l), f_2 (n , number of nodes; i , number of node freedom) and f_3 , respectively. While the member-related design constraints (MRDC) along with the joint-related design constraints

$$\begin{aligned}
 P_1 &= \left(\sum_{k=1}^m (w.l)_k \right) \cdot (CGN \cdot \varphi)^{\frac{1}{(P_{Mem} + P_{Joint} + P_{Disp})}} \\
 P_2 &= \min(d_{ij}) \cdot (CGN \cdot \varphi)^{\frac{1}{(P_{Mem} + P_{Joint} + P_{Disp})}} \\
 P_3 &= \max(f_{ij}) \cdot (CGN \cdot \varphi)^{\frac{1}{(P_{Mem} + P_{Joint} + P_{Disp})}}
 \end{aligned}
 \left\{ \begin{aligned}
 P_{Mem} &= \sum_{k=1}^m p_k, \begin{cases} p_k = 1 \text{ if } Member_Strength_Constraints \geq 1 \\ p_k = 0 \text{ if } Member_Strength_Constraints < 1 \end{cases} \\
 P_{Joint} &= \sum_{k=1}^m p_k, \begin{cases} p_k = 1 \text{ if } Joint_Strength_Constraints \geq 1 \\ p_k = 0 \text{ if } Joint_Strength_Constraints < 1 \end{cases} \\
 P_{Disp} &= \sum_{j=1}^n \sum_{i=1}^{12} p_d^{ij} \begin{cases} p_d^{ij} = 1 \text{ if } Unity_{Disp}^{ij} \geq 1 \\ p_d^{ij} = 0 \text{ if } Unity_{Disp}^{ij} < 1 \end{cases}
 \end{aligned} \right. \quad (4)$$

$$Member_Strength_Constraints = \begin{cases} Unity_{Axial}^k, Unity_{Bending}^k, Unity_{CombinedBending}^k, Unity_{Shear}^k, \\ Unity_{Torsion}^k, Unity_{AxialCompr \& BendingBuck}^k, Unity_{Axial \& BendingYield}^k \end{cases} \quad (5)$$

$$Joint_Strength_Constraints = \begin{cases} Unity_{JointYield}^k, Unity_{JointAxial}^k, Unity_{JointBending}^k, Unity_{JointAxial \& Bending}^k, \\ Unity_{JointStrength}^k, Unity_{JointSpecialControl1}^k, Unity_{JointSpecialControl2}^k \end{cases} \quad (6)$$

Table 1 Three Geometrical Configurations Used to Arrangement of Arched and Diagonal Members for Sphere and Ellipse Shaped Dome Structures

	Geometrical Configuration 1	Geometrical Configuration 2	Geometrical Configuration 3
Cross-sectional Properties of Longitudinally Arched Members	Same	Different	Different
Cross-sectional Properties of Horizontally Arched Members	Different	Different	Different
Cross-sectional Properties of Diagonal Members	Not Included	Different	Not Included

(JRDC) are represented by $Unity_{Axial}$, $Unity_{Bending}$, and etc. along with $Unity_{JointAxial}$, $Unity_{JointBending}$ and etc. respectively, the nodal displacement-related design constraint are defined by $Unity_{Disp}$ (Eq. (4)). The terms, current generation number CGN and φ in Eq. (4) are dynamically adjusted depending on the generation number (see the further details about the use of these parameters in Reference [21]). In case of exceeding one of the constraint-related upper limit values, this unsatisfactory result is penalized by the penalty values P_1 , P_2 and P_3 (Eqs. (4–6)). It is noted that the extended details of MRDC and JRDC in Eqs. (5–6) are presented in [20, 22].

PAGA is employed for the design optimization of sphere and ellipse shaped SDS considering the provisions of API RP2A-LRFD specification. Firstly, the three type configurations of sphere and ellipse-shaped SDS are automatically generated by an intelligent dome generating tool and analyzed for structural responses using a geometrically nonlinear structural analysis approach named arc length method (see Table 1). For this purpose, ANSYS program is utilized to perform the nonlinear structural analysis. The basic governing parameters of arc length method are convergence tolerance that determines the completion of incremental-iterative loop, load step numbers that specifies the number of sub-steps to be taken the current load

step, arc length multiplier that determines maximum multiplier of the reference arc-length radius (see their assumed values in Table 2). Then, the structural responses are utilized to check the efficiencies of joint and member-related strength capacities of SDS. For this purpose, the current strengths of dome members and the allowable nominal strengths are easily computed. However, the main difficulty is the inclusion of these strength-related computations into the proposed optimization algorithm. In order to overcome this barrier, a ratio of available strength of dome member to the allowable nominal strength along with a ratio of maximum value of nodal displacement to a pre-assumed value are utilized. These ratios are named *Unity* in this study. Thus, it is possible to include each of these values of *Unity* into the proposed optimization algorithm as a design constraint. A checking procedure through the value of unity is performed for the violation of each different design constraints. At this point, the main distinguished feature of the proposed optimal design procedure is its flexibility of integrating the geometric nonlinearity by one of the available specification provisions. The three type configurations of sphere and ellipse-shaped SDS are generated depending on the topology, shape and size-related design variables. While the basic parameters that are utilized to define the proposed dome configurations are

Table 2 Design Variables and Values Governed The Proposed Optimal Design Approach

Design Variable Names	Design Variable Values	
Size Related Design Variables	Varying Design Variables	Fixed Design Variables
Par_{DVL}		$Par_{DVL} = 1 < Par_{DVU} = 37$
Shape Related Design Variables		
Par_{SDVx}	$Par_{SDVxL} = 19m < Par_{SDVxU} = 21m$	$Par_{SDVxL} = Par_{SDVxU} = 20m$
Par_{SDVy}	$Par_{SDVyL} = 19m < Par_{SDVyU} = 21m$	$Par_{SDVyL} = Par_{SDVyU} = 20m$
Par_{SDVz}	$Par_{SDVzL} = 19m < Par_{SDVzU} = 21m$	$Par_{SDVzL} = Par_{SDVzU} = 20m$
Topology Related Design Variables		
Par_{LDNL}		$Par_{LDNL} = 2 < Par_{LDNU} = 5$
Par_{HDNL}		$Par_{HDNL} = 2 < Par_{HDNU} = 5$
Structural Analysis Related Parameter Names	Structural Analysis Related Parameter Values	
Convergence Tolerance (see CNVTOL)	0.00001	
Load step (see NSUBST)	500	
Arc-length mult. (see ARCLen)	50	

presented in the Table1, their values along with the parameter values of structural analysis approach are tabulated in Table 2. In this regard, the shape-related design variables Par_{SDVx} , Par_{SDVy} and Par_{SDVz} which are limited by the upper and lower values Par_{SDVxL} , Par_{SDVxU} and etc. indicates the height and spanning distances of ellipse and sphere shaped SDS. The topology-related design variables Par_{LDNL} and Par_{HDNL} which are limited by the upper and lower values Par_{LDNL} , Par_{LDNU} and etc. indicates the longitudinal-horizontal division numbers for SDS. Although the sphere and ellipse shapes of SDS are fixed throughout the evolutionary search, the numbers of horizontal and longitudinal members are consistently altered depending on the topology-related design parameters Par_{LDNL} and Par_{HDNL} . Thus, the change in the relative nodal position of SDS causes to a variation in the geometrical configuration SDS. It is clear that an increase in the number of topology-related design variables elevates the similarity degree between the resulted geometrical configuration and the actual sphere or ellipse shapes. The size-related design variables Par_{DVL} which is limited by the upper and lower values $Par_{DVL} = 1$ and $Par_{DVU} = 37$ indicates the properties of 37 different circular hollow cross-sections. The design grouping for size-related design variables is carried out depending on the arrangement of SDS elements. Thus, three different sizes are automatically assigned to the horizontal, longitudinal and diagonal members by the proposed dome generating tool. The cross-sectional properties of SDS members are assigned from the lists of ready hot-rolled profiles with tubular cross-sectional shapes due to their higher resisting capacity to the torsion-related effects compared to the open cross-sections. The tubular members of SDS with circular hollow cross-sections are named as "cylindrical member" in API RP2A-LRFD specification. The structural strength

and stability requirements for the cylindrical members are specified in the section "D" of API RP2A-LRFD specification. Cylindrical member-related design provisions of API RP2A-LRFD specification is summarized in Table 3 including the equation numbers in the proposed specification. Although the application details of design provisions employed for MRDC are relatively clear due to existence a direct relation to the members of SDS, the design provisions employed for JRDC is required a further consideration due to the determination of joint-related strength capacities depending on both members and joints of SDS. Therefore, the further details about JRDC are presented in following parts.

The cylindrical members of SDS, each of which are defined as "chord" and "brace" in API RP2A-LRFD specification are connected at any joint without overlap of principal braces, having no-gussets, diaphragms or stiffeners (see Fig. 2). Therefore, a joint used to connect chord and brace members of SDS is named as "tubular joint" in API RP2A-LRFD specification (see Fig. 4). The code provisions for the tubular joints in API RP2A-LRFD specification are arranged according to three sub-categories:

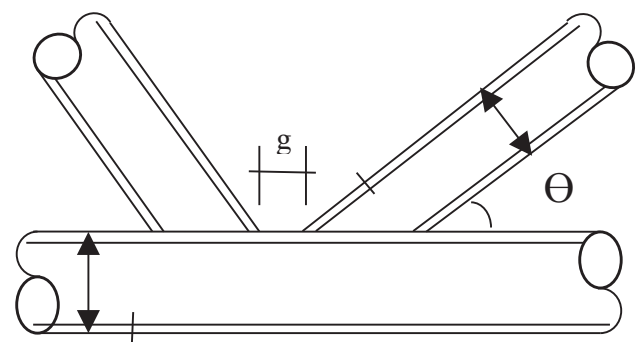


Fig. 4 Geometric Design Parameters for Tubular Joint Connections

i) **Joint Classification:** There exists a possibility of being chord cylindrical members in both the horizontal and longitudinal directions. The variation in geometry of tubular joints leads to a categorization of three main classes "K, T and Y". Firstly, the cylindrical member with a larger diameter is assigned as chord member. Then, brace members are attached to the chord member. Thus, while the tubular joint named "T" is defined for the case of being the brace member "perpendicular" to the chord member, a non-perpendicular brace is used to define for the tubular joint "K". The other important requirement in the specification of API RP2A-LRFD is related to the amount of angle between chord and brace members. The value of angle has to be higher than 20 degree (see Θ in Fig. 2) in order to adequately satisfy for the tubular joint capacity. These requirements are included into current JRDC as "Special Control1" and "Special Control2" in order to check the both existence of chord brace and the amount of angle, respectively (see Eq. 6).

ii) **Joint Capacity:** The effective strength is determined depending on the yield strengths of brace and chord cylindrical members along with "joint geometry-related parameters", such as diameters, thickness, of chord and brace cylindrical members and etc. Therefore, the existence of brace and chord member is one of the most important checks for the determination of joint strengths.

The strength check of tubular joints is carried out comparing the factored joint axial and bending forces with the ultimate joint axial and bending capacities. The ultimate joint axial and bending capacities (see the provisions of AP RP2A-LRFD specification) are determined depending on the design parameters named "ultimate strength factor" and "design factor". The ultimate strength factor is tabulated in consideration of the joint geometry-related parameters along with the forces of axial, tension and in-plane & out-plane bending (see the provisions of AP RP2A-LRFD specification). The design factor is computed using both the values of factored axial, in-plane & out-plane bending stresses in chord and some fixed values (0.030 for brace axial stress, 0.045 for brace in-plane bending stress, 0.021 for brace out-plane bending stress. Furthermore, a strength check against the combination of axial and bending loads in brace is also included into the provisions of API RP2A-LRFD specification for the tubular joints

iii) **Joint Strength:** the tubular connections should have a sufficient strengths which is not less than %50 of the effective strength of cylindrical member.

Tubular joint-related design provisions of API RP2A-LRFD specification is summarized in Table 4 including the equation numbers in the proposed specification.

Table 3 A Summary for The Proposed Member-related Design Constraints

	Axial Tension Stress	Bending Stress	Axial Compress. Stress	Shear Stress	Torsional Shear Stress	Names of Unity Check
Nominal Yielding Strength	D.2.1-1	-	-	-	-	Axial (Tension Related) Unity Check
Nominal Axial Compress. Strength	-	-	D.2.2-1	-	-	Axial (Compress. Related) Unity Check
Nominal Bending Strength	-	D.2.3-1	-	-	-	Pure Bending Unity Check
Nominal Shear Strength	-	-	-	D.2.4-1	-	Flexural Shear Unity Check
Nominal Torsional Strength	-	-	-	-	D.2.4-3	Torsional Shear Unity Check
Combined Axial Tension and Bending Strength	D.3.1-1	-	-	-	-	Combined Axial and Bending Yield Unity Check
Combined Axial Compress. and Bending Strength	-	D.3.2-(2-3)	-	-	-	Combined Axial and Bending Yield Unity Check
Nominal Axial Compress. Strength (Euler Buckling)	-	-	D.2.2.-(2a,2b,2c)	-	-	Elastic Buckling Unity Check
Combined Axial Compress. and Bending For Buckling Strength	-	D.3.2-1	-	-	-	Combined Axial and Bending Related Buckling Unity Check

Table 4 A Summary for The Proposed Joint-related Design Constraints

	Joint Geometry Related Parameters	Yield Strength of Chord and/or Brace	Chord Design Factor	Ultimate Strength Factor	Names of Unity Check
Joint Strength		E.3.1			Joint Strength Unity Check
Ultimate Joint Axial Capacity			E.3.5		Axial Force Unity Check
Ultimate Joint Bending Moment Capacity			E.3.6		Bending Moment Unity Check
Combined Joint Axial and Bending Capacity			E.3.4		Combined Joint Axial and Bending Unity Check
Special Control	Angle between chord and brace (>20)				A Special Control for Brace-Chord Angle Lower Than 20
Special Control	Chord or Brace has to be exist				A Special Control for Existence of Brace-Chord

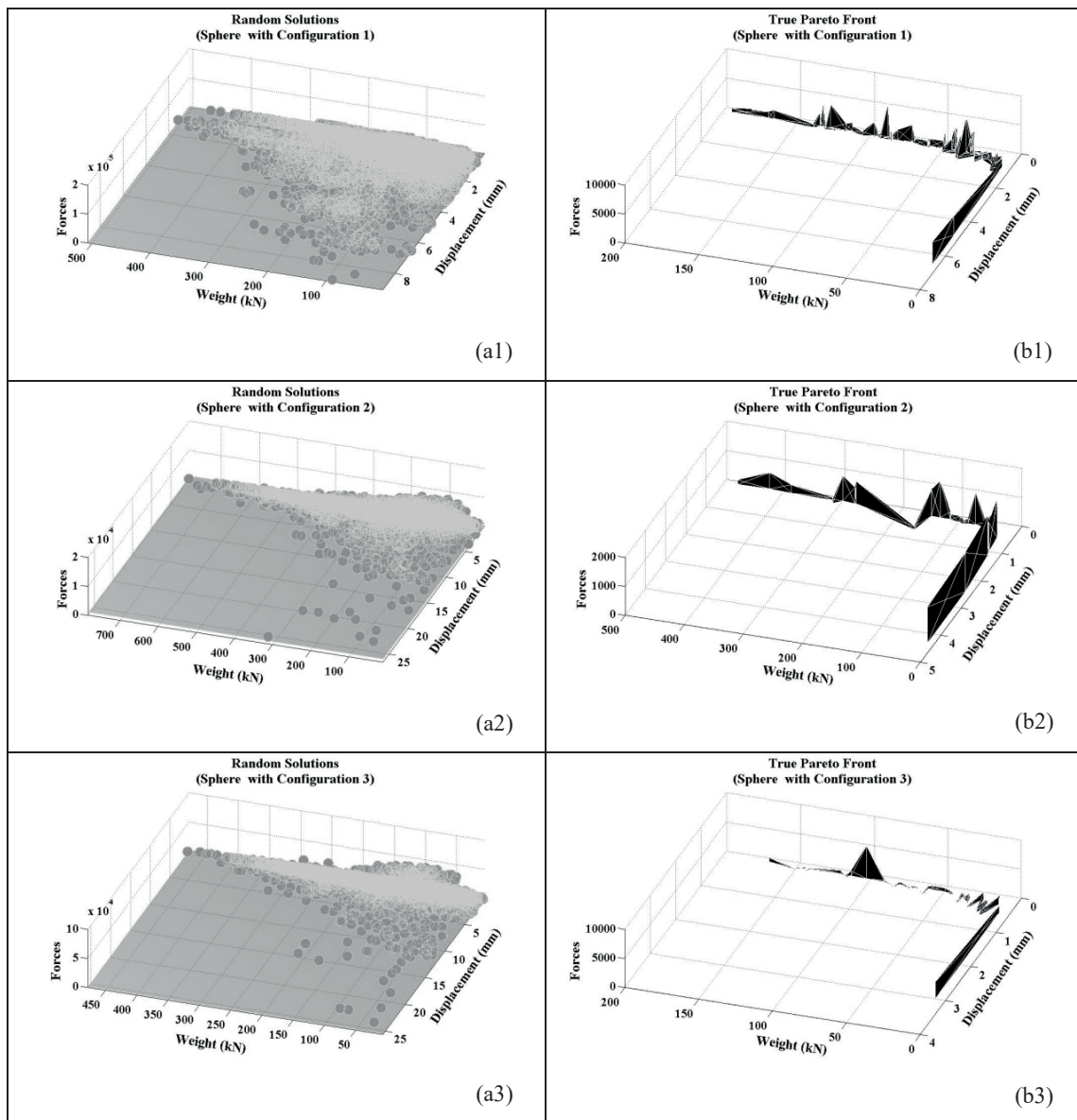


Fig. 5 True Pareto Front and Random Solutions (Sphere-shaped Dome Structure with Geometrical Configurations 1 (a1–b1), Geometrical Configurations 2 (a2–b2) and Geometrical Configurations 3 (a3–b3))

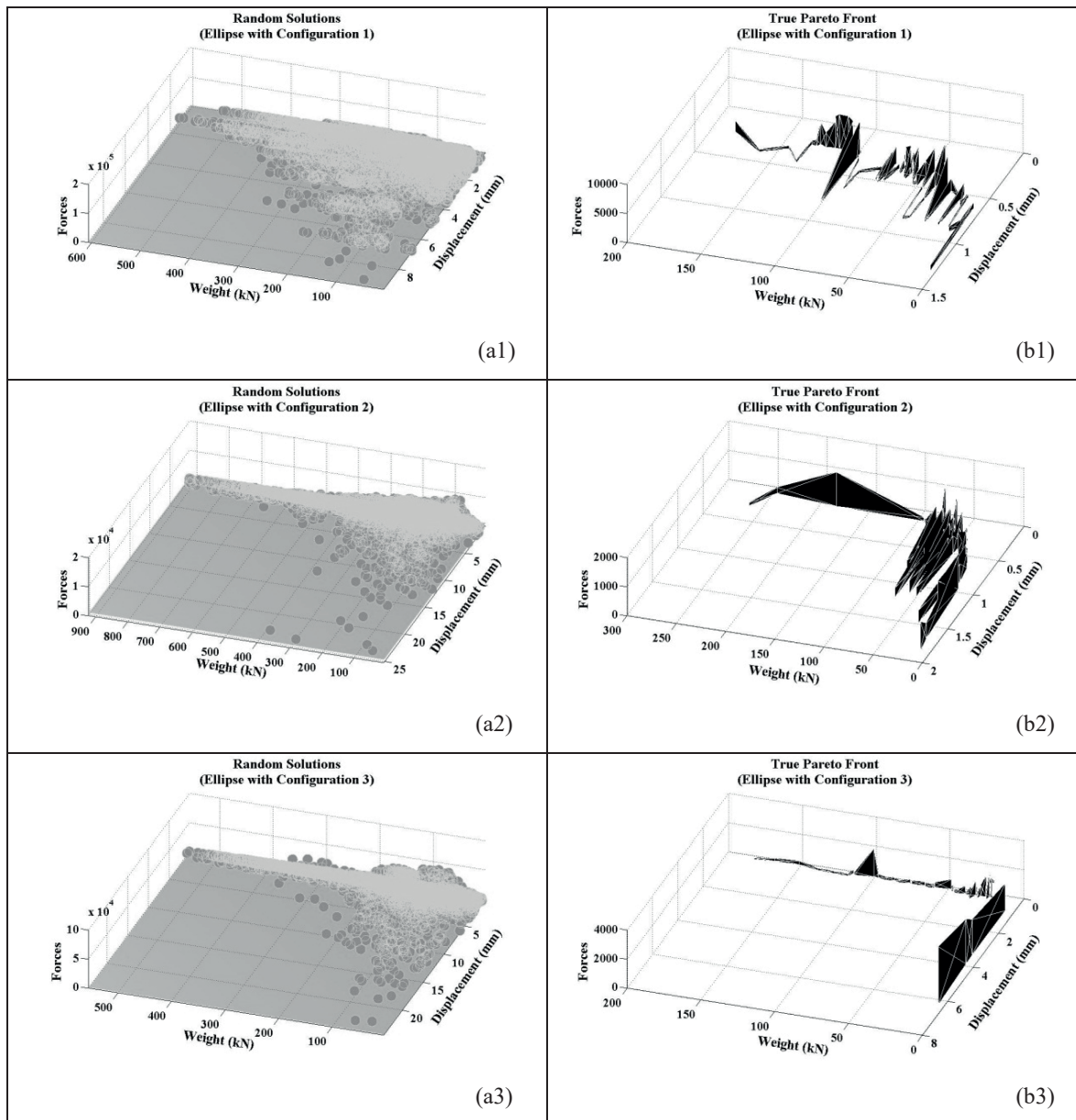


Fig. 6 True Pareto Front and Random Solutions (Ellipse-shaped Dome Structure with Geometrical Configurations 1 (a1–b1), Geometrical Configurations 2 (a2–b2) and Geometrical Configurations 3 (a3–b3))

3 Discussion of results

In the Section 2, it is mentioned that the design of SDS is optimized considering the displacement-related design constraints and different cases of MRDC and JRDC which have responsibility of checking the efficiencies of both cylindrical member and tubular joint capacities according to the provisions of API RP2A-LRFD specification. Each of design constraints is numerically represented by a unity value (see the Eqs. 5–6). Thus, it is possible to investigate not only the unity values of MRDC and JRDC but also the values of objective functions are computed at each displacement increment.

The proposed optimal design procedure is applied into a design example which was optimized using only MRDC [21]. In this study, the same design example is firstly optimized considering both MRDC and JRDC. Then, the quality of objective functions are examined. Thus, it is possible to determine the dominant design constraints for the cases of both MRDC and JRDC. However, both the increased number of objective functions and variety in the cases of MRDC and JRDC makes a difficulty in the determination of dominant design constraints. Therefore, the best way in the evaluation of optimal designs is to use an average value or normalized average value of both the objective function values

and unity values of MRDC and JRDC. For this purpose, the incremental step numbers of the nonlinear structural analysis is limited to an upper value "10". It is noted that the value of unity for the proposed design constraints being higher than "1.0" means a constrained-related violation. Therefore, the values of unity being lower than "1.0" are utilized to indicate a "satisfactory degree" for the displacement-related design constrain and the cases of MRDC and JRDC.

In this framework, the optimal designs are evaluated in three sub-sections:

3.1 The evaluation of objective functions with regard to the incremental step numbers of geometrically nonlinear structural analysis

The average value of each objective function is firstly computed for at each incremental load step and then stored for a further consideration. The values of objective functions are depicted to display both the true pareto fronts and pareto fronts (see Figs. (5–6)). Thus, it is possible to depict the average values of minimum entire weights and joint displacements along with the maximum member force of SDS using a bar chart for SDS with both sphere and elliptical-types (see Figs. (7–9)). These illustrations provide a big advantage for both a solely and an interacted comparison of objective function values throughout the numbers of incremental steps of nonlinear structural analysis which is located in the x axis of each figure.

Considering Figs. (7–9) along with Figs. (5–6), the following results are drawn:

1. It is seen that the violation of MRDC and JRDC generally begins at the incremental step number "3" and "4" and ends at the incremental step number "7" and "10" of nonlinear structural analysis approach, respectively. Particularly, the JRDC for the SDS with configuration 2 is violated at the minimum incremental step number "5" and the maximum one "10" (see Figs. (7–9)).
2. As an expected, using the ready hot-rolled profiles with larger size in the construction of SDS leads to an increase in the incremental step number of nonlinear structural analysis approach. This result is easily seen from the increased peaks toward the end of incremental steps of nonlinear structural analysis in Fig. (7).
3. It is clear that an increase in the entire weight of SDS, in other words, the use of ready hot-rolled profiles with larger size for SDS plays a big role to prevent the violation of MRDC rather than JRDC (see the increased peaks corresponding to the cases of MRDC

and JRDC in Fig. (7)). However, there also exists an evidence showing JRDC to be an important design factor as much as MRDC (see the bars with equal heights for the cases of MRDC and JRDC in the Fig. (7))

4. In order to obtain an optimal design with a higher load-carrying capacity, using the ready hot-rolled profiles with larger size has a big importance in order to prevent the violation of both MRDC and JRDC for SDS with sphere and ellipse-type geometrical configuration 2 (see Figs. 9(a2) and 9(b2) along with Figs. 7(a2), 7(b2)).
5. The other interesting result is concerned with the ductility issue which informs about the energy absorption capacity of SDS. Thus, the increased nodal displacements point out a higher ductility capacity of SDS. It is clear that the increase in the entire weight of SDS leads to a higher increase in the ductility capacity of SDS with sphere and ellipse shaped geometrical configuration 2 (see Figs. 8(a2) and 8(b2) along with Figs. 7(a2) and 7(b2)).
6. The design of SDS with ellipse type geometrical configuration 2 is resulted by the highest weight, nodal displacement and forces with respect to other design of SDS with different geometrical configurations (Table 5). SDS with ellipse type geometrical configuration 1 has relatively lower weight, nodal displacement and forces than the SDS with ellipse type geometrical configuration 3. This result shows that the ductility and load-carrying capacities of SDS with ellipse type geometrical configuration 3 are higher than SDS with ellipse type geometrical configuration 1 but lower than SDS with ellipse type geometrical configuration 2.

Table 5 The Ranks of Objective Functions According to Proposed Geometrical Configurations

Ranking Order (from Max. to Min.)	Weight Values (mm)	Nodal Displacements (kN)	Nodal Forces (kN)
1.1	Ellipse Geom. Con. 2	Ellipse Geom. Con. 2	Ellipse Geom. Con. 2
1.2	Sphere Geom. Con. 2	Sphere Geom. Con. 2	Sphere Geom. Con. 2
2.1	Ellipse Geom. Con. 3	Ellipse Geom. Con. 3	Ellipse Geom. Con. 3
2.1	Sphere Geom. Con. 3	Sphere Geom. Con. 3	Sphere Geom. Con. 3
3.1	Ellipse Geom. Con. 1	Ellipse Geom. Con. 1	Ellipse Geom. Con. 1
3.2	Sphere Geom. Con. 1	Sphere Geom. Con. 1	Sphere Geom. Con. 1

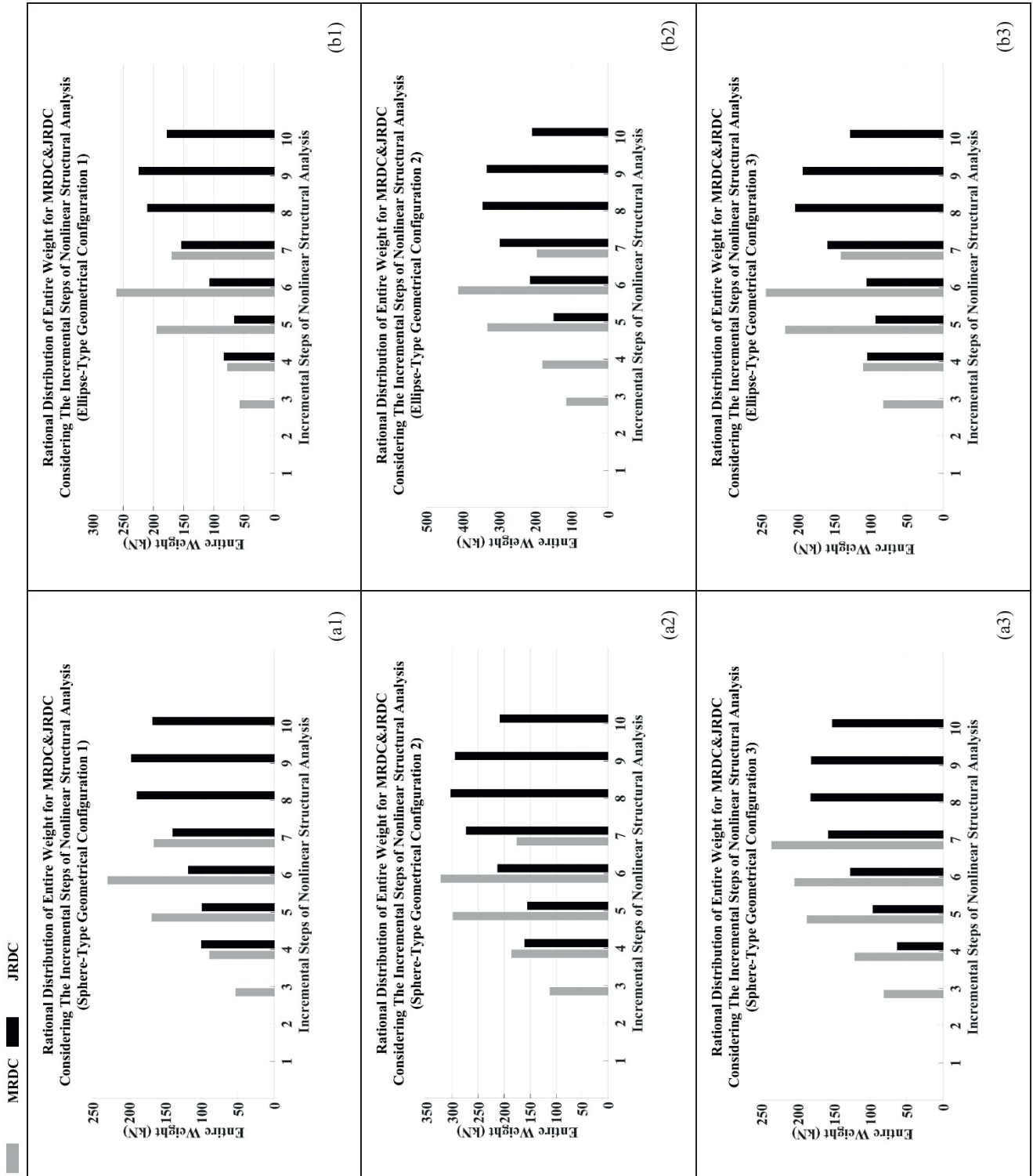


Fig. 7 Rational Distribution of Entire Weight of SDS Considering Unity Value for The Cases of MRDC&JRDC throughout Incremental Steps of Nonlinear Structural Analysis (Sphere and Ellipse-shaped Dome Structure with Geometrical Configurations (1–3))

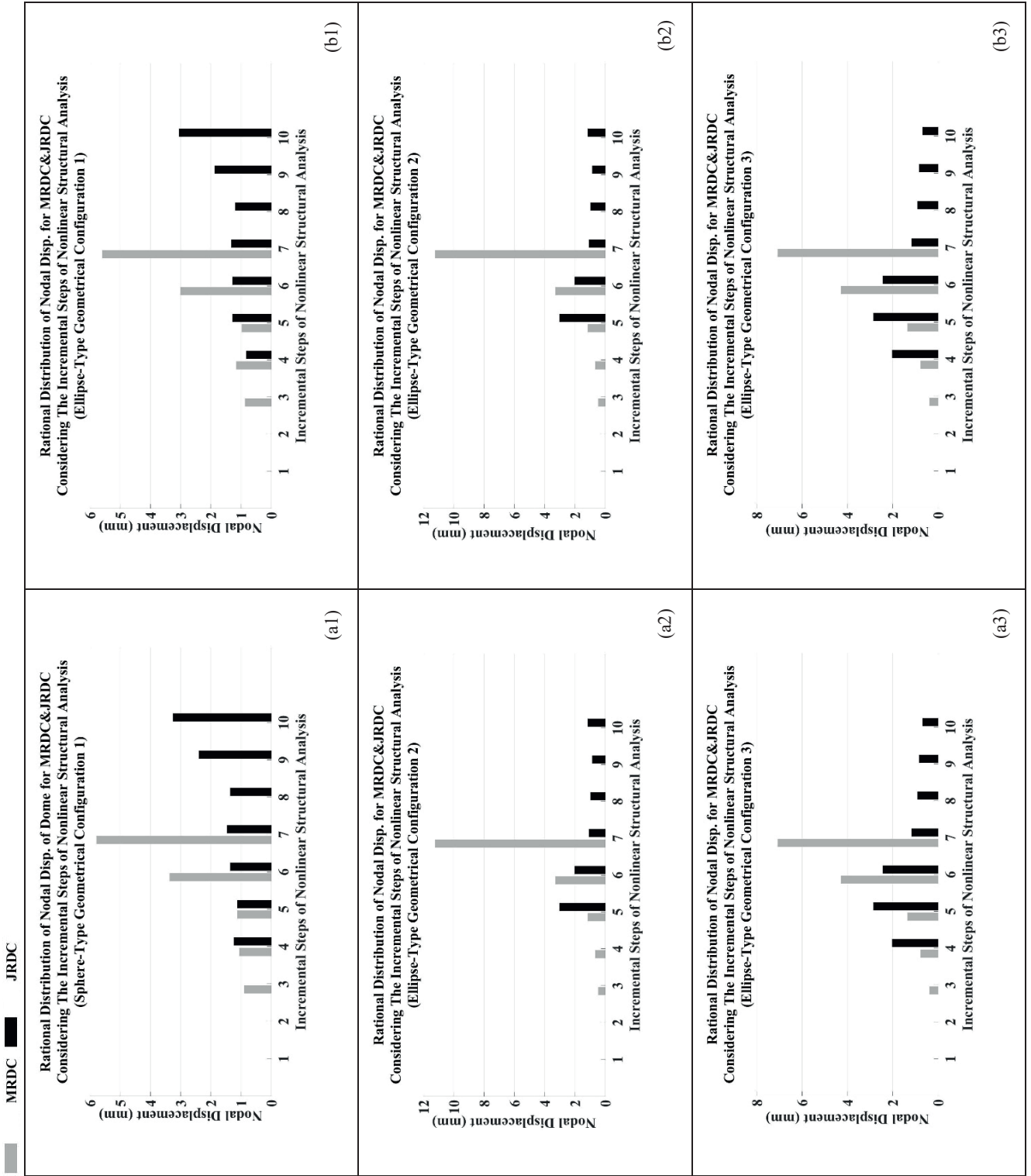


Fig. 8 Rational Distribution of Nodal Displacements of SDS Considering Unity Value for The Cases of MRDC&JRDC throughout Incremental Steps of Nonlinear Structural Analysis (Sphere and Ellipse-shaped Dome Structure with Geometrical Configurations (1–3))

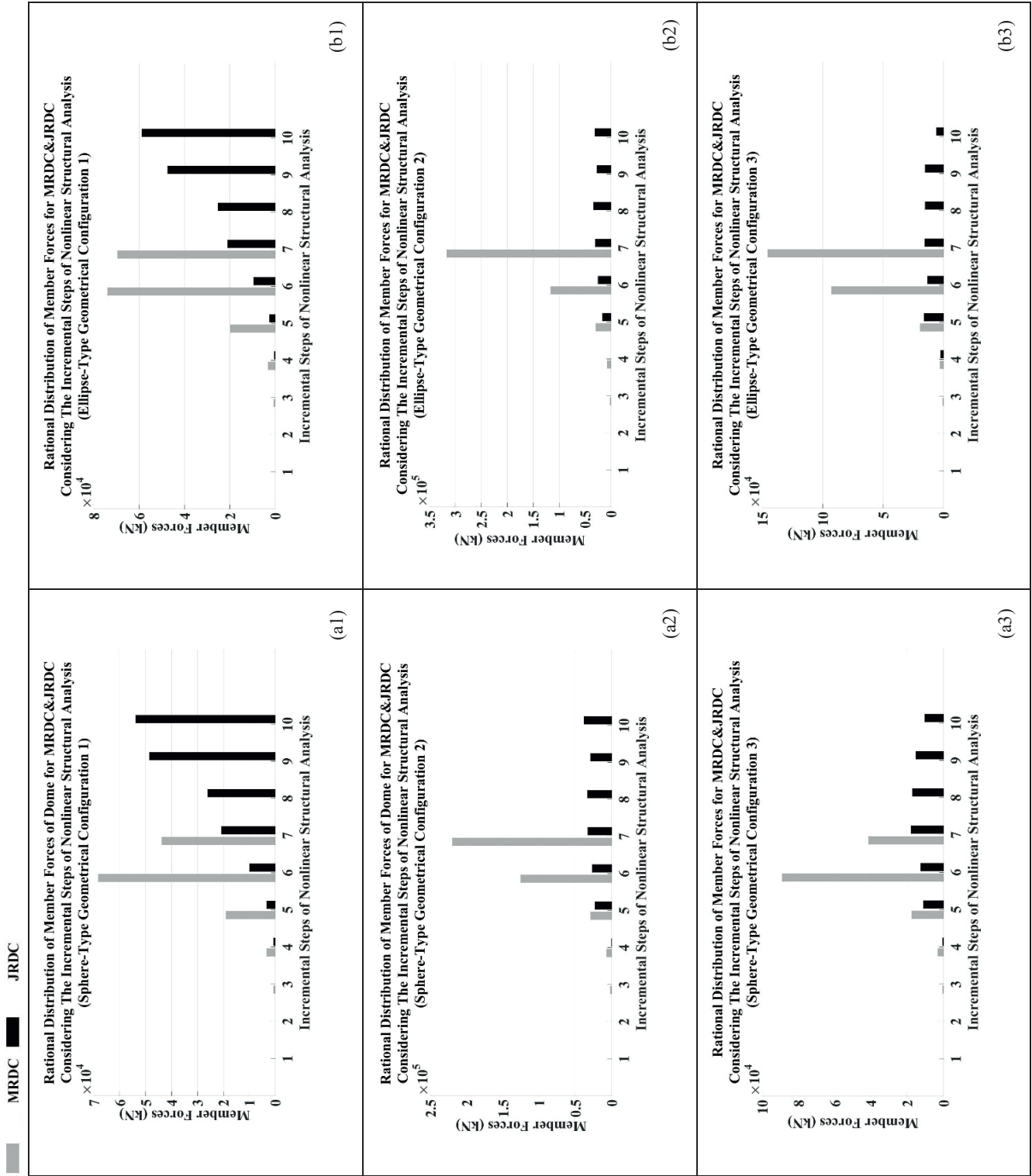


Fig. 9 Rational Distribution of Member Forces of SDS Considering Unity Value for The Cases of MRDC&JRDC throughout Incremental Steps of Nonlinear Structural Analysis (Sphere and Ellipse-shaped Dome Structure with Geometrical Configurations (1–3))

3.2 The evaluation of member and joint-related design constraints

In this sub-section, the design constraints for the cases of MRDC and JRDC are evaluated comparing with each other's. Thus, it is possible to determine the dominant ones for the cases of MRDC and JRDC. Nothing that the value of unity for the cases of MRDC and JRDC being higher than "1.0" informs about a violating occurrence, the values of unity which are lower than "1.0" are stored. Then, their average values are computed for the six cases of MRDC and five cases of JRDC, respectively. Then, these categorized average values of related values of unity are normalized for each case of MRDC and JRDC, separately. These normalized & categorized average values of unities are indicated by "value of unity" in figures. Thus, their sum for each cases of MRDC and JRDC correspondingly equals to "1.0" (see Figs. (8–9)).

The names of dominant design constraints considering the violation of MRDC are ranked in an order of "elastic-buckling", "combined axial and bending yield" and "axial (tensional)", respectively (see their higher unity values in Figs. 10(a1–a3)). Particularly, the design constraint named "elastic-buckling" is more sensitive in the design of SDS with both and sphere and ellipse type geometrical configuration 3 due to the lack of diagonal members (see the higher values of unities in Figs. 8(a3) and 8(b3)).

The names of dominant design constraints considering the violation of JRDC are firstly "combined axial and bending" and then "special control for existence of chord brace", "axial force", "joint strength" and "a special control for brace angle lower than 20 degree", respectively (see Figs. 11(a1–a3) and 11(b1–b3)). Particularly, the design constraints named "combined axial and bending" along with "a special control for existence of chord brace" are more sensitive in the design of SDS with both and sphere and ellipse type geometrical configuration 3 due to the lack of diagonal members (see the higher value of unity in Figs. 11(a3) and 11(b3)).

3.3 The evaluation of design constraints considering the horizontal and longitudinal division numbers

In this sub-section, the design constraints are evaluated thereby categorizing according to both the horizontal and longitudinal division numbers. The values of unity which are lower than "1.0" along with both the horizontal and longitudinal division numbers are stored. Then, the average values of unities corresponding to the six cases of MRDC and five cases of JRDC are stored for each horizontal and

longitudinal division numbers. These categorized average values of related unity are normalized for each horizontal and longitudinal division numbers. Thus, a normalized & categorized average value is indicated with "value of unity" in figures. Thus, the sum of these unity values for each horizontal and longitudinal division numbers correspondingly equals to "1.0" (see Figs. 12–15).

Considering both horizontally and longitudinally division numbers, the names of dominant design constraints for the cases of MRDC are ranked in an order of "elastic buckling", "combined axial and bending", "axial (tensional) force" and "flexural shear", respectively (see their higher unity values in Figs. 12(a1–a3), 12.(b1–b3), Fig 13(a1–a3) and 13(b1–b3)). The design constraint named "combined axial compression and bending-related buckling" is never seen in these Figures. Particularly, the design constraint named "flexural shear" is observed in either a lower value or "0" for the SDS with both sphere and ellipse type geometrical configurations 1 and 3 (see Figs. 12(a1 and a3), 12(b1 and b3), 13(a1 and a3) and 13(b1 and b3)). The value of unity for design constrain named "combined axial and bending yield" is increased depending on an elevation in both horizontally and longitudinally division numbers.

The order of dominant design constraints for the cases of JRDC is ranked as "combined axial and bending", "a special control for existence of chord brace", "a special control for angle lower than 20 degree", "axial force" and "joint strength", respectively (see Figs. 14(a1–a3), 14(b1–b3), 15(a1–a3) and 15(b1–b3)).

Due to the lack of diagonal members, an increase in the unity value of design constraint named "a special control for existence of chord brace" as a case of JRDC is resulted by a higher value for the design of SDS with both and sphere and ellipse type geometrical configuration 3. (see Figs. 14(a3 and b3) and 15(a3 and b3)).

A decrease in both horizontally and longitudinally division numbers causes to an increase in the unity values corresponding to the different cases of JRDC and MRDC (see Figs. 14(a1–a3), 14(b1–b3), 15(a1–a3) and 15(b1–b3)).

4 Conclusions

This study firstly introduces the emergence of proposed optimal design approach for the geometrically nonlinear SDS. It is emphasized that utilizing an optimization procedure with multiple objectives and compact design specification has a big importance on the optimal design of SDS. Particularly, it is also mentioned that involving a compact design specification into the design stage gives

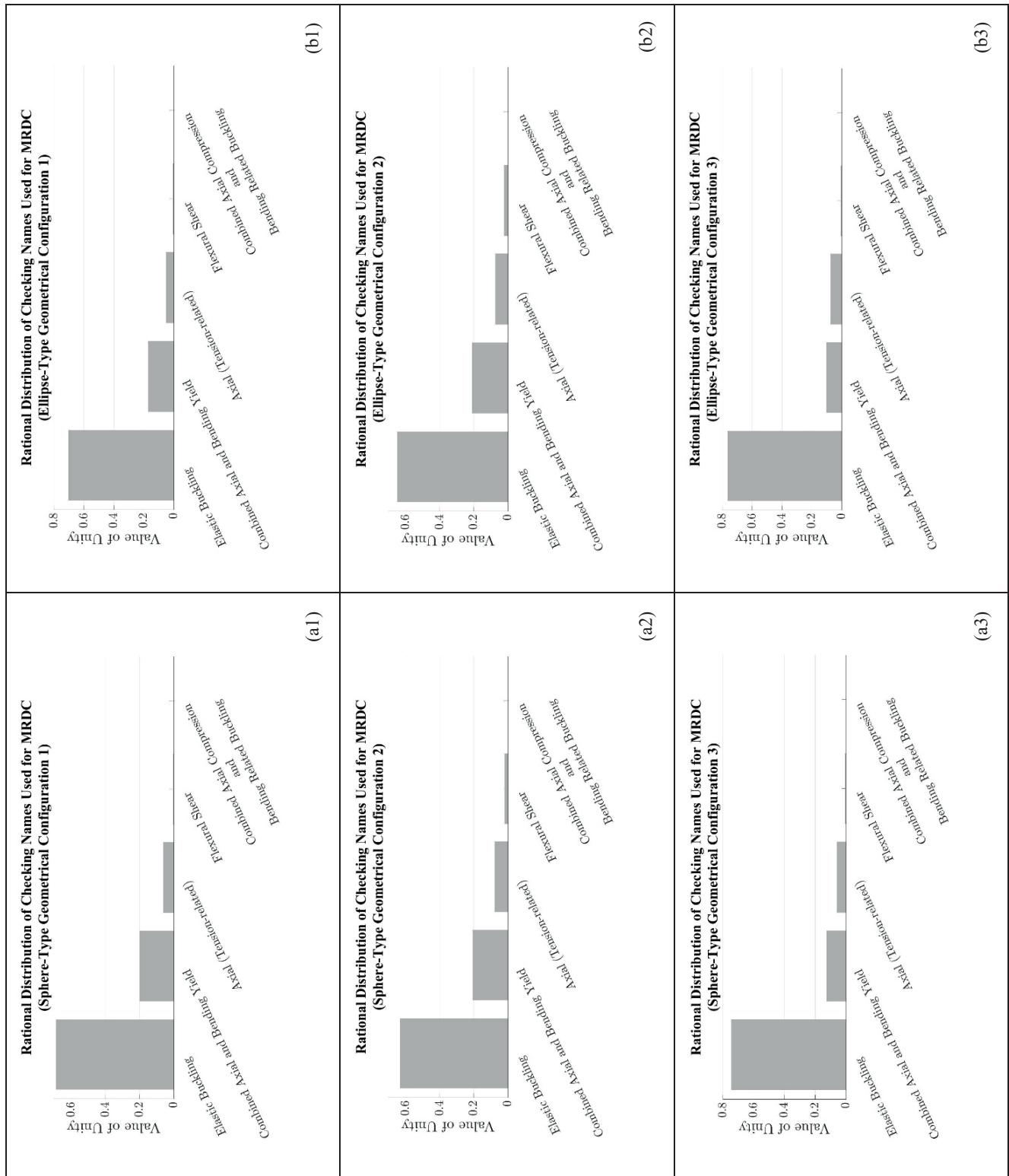


Fig. 10 Rational Distribution of Unity Value for The Cases of MRDC throughout Checking Names (Sphere and Ellipse-shaped Dome Structure with Geometrical Configurations (1–3))

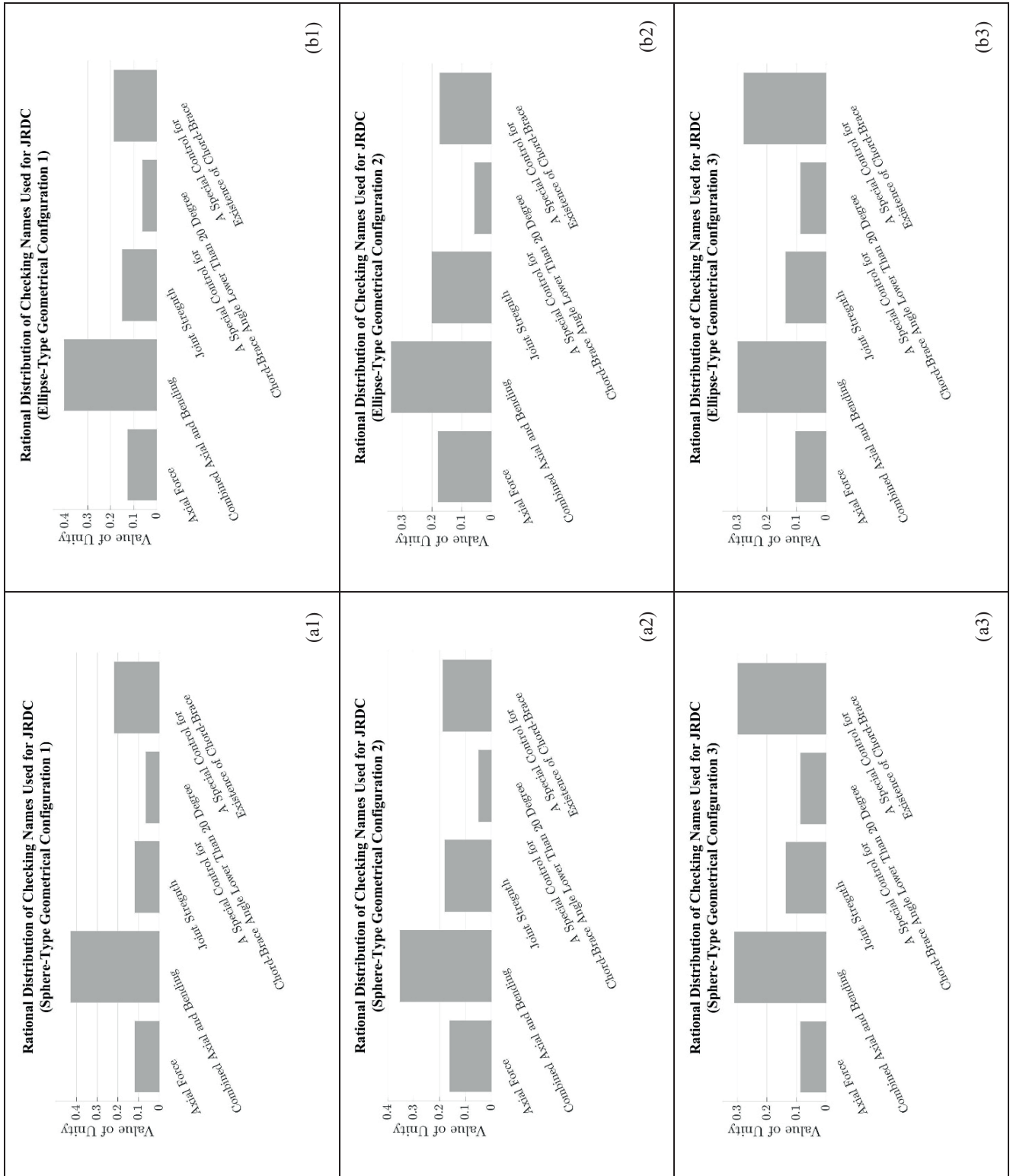


Fig. 11 Rational Distribution of Unity Value for The Cases of JRDC throughout Checking Names (Sphere and Ellipse-shaped Dome Structure with Geometrical Configurations (1-3))

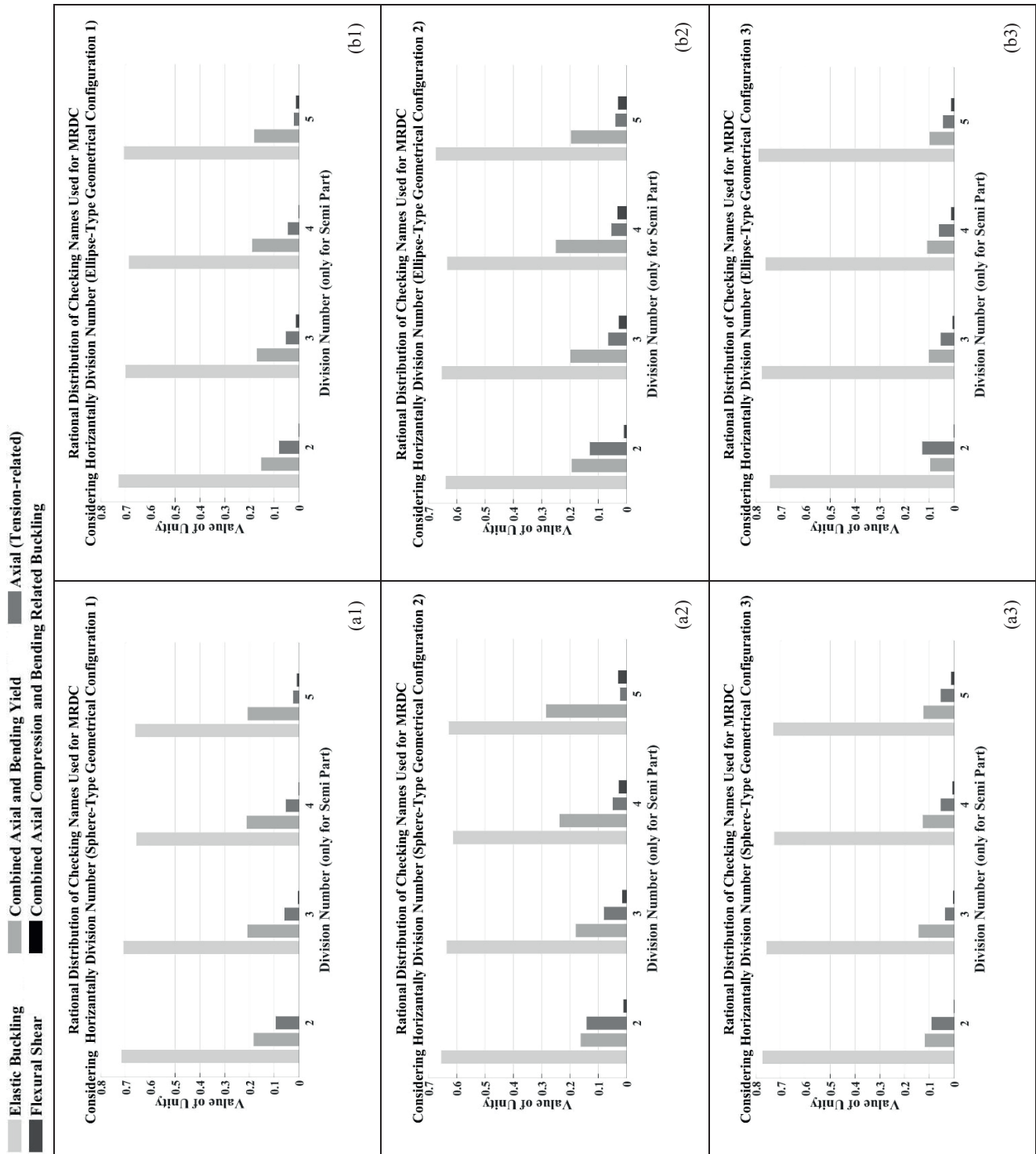


Fig. 12 Rational Distribution of Unity Value for The Cases of MRDC throughout Horizontally Division Numbers (Sphere and Ellipse-shaped Dome Structure with Geometrical Configurations (1–3))

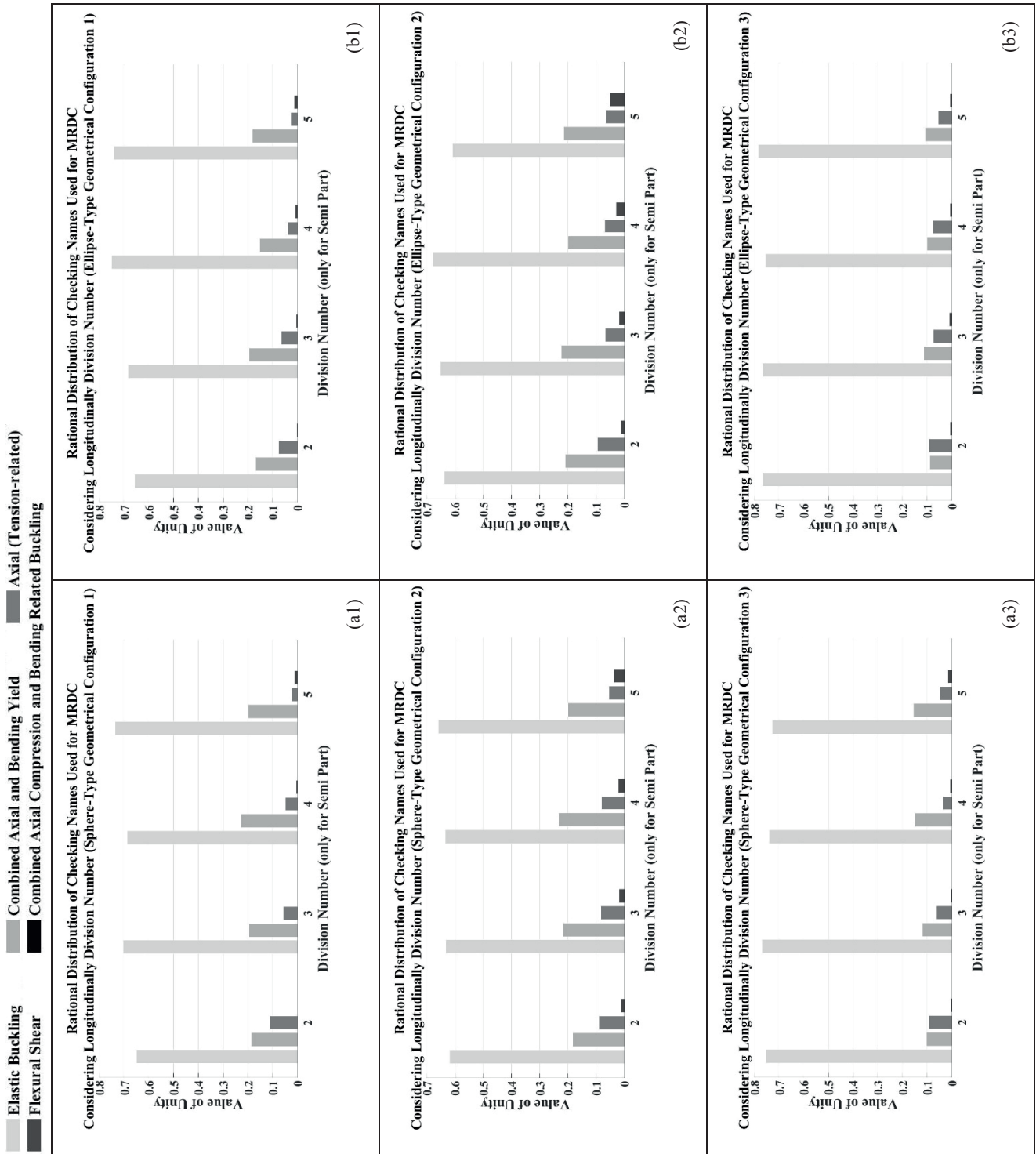


Fig. 13 Rational Distribution of Unity Value for The Cases of MRDC throughout Longitudinally Division Numbers (Sphere and Ellipse-shaped Dome Structure with Geometrical Configurations (1–3))

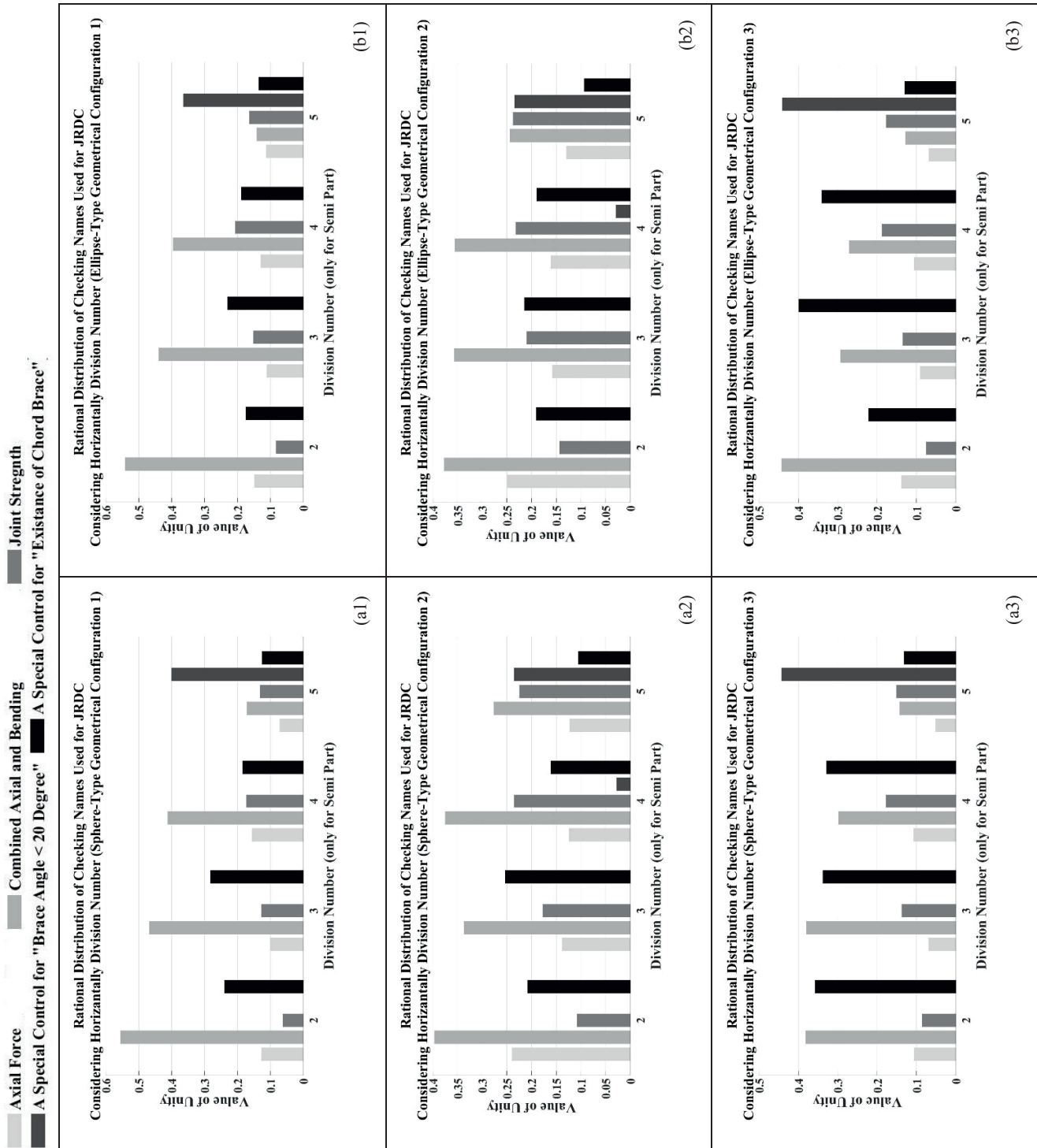


Fig. 14 Rational Distribution of Unity Value for The Cases of JRDC throughout Horizontally Division Numbers (Sphere and Ellipse-shaped Dome Structure with Geometrical Configurations (1–3))

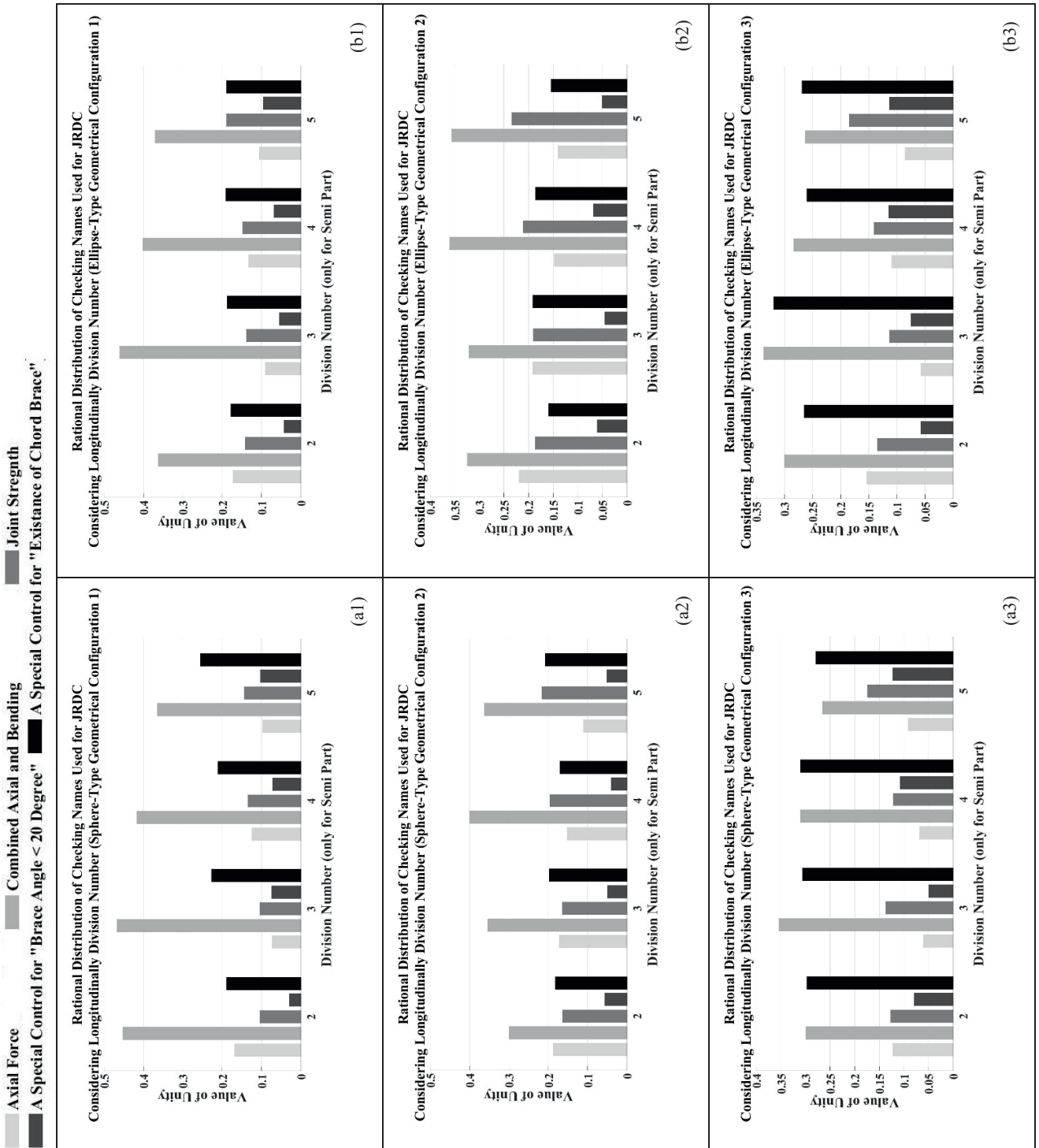


Fig. 15 Rational Distribution of Unity Value for The Cases of JRDC throughout Longitudinally Division Numbers (Sphere and Ellipse-shaped Dome Structure with Geometrical Configurations (1–3))

the designer an opportunity for investigating the effects of different cases of JRDC and MRDC on the optimal designs and determining the most appropriate design according to the preference of designer.

In this framework, the values of objective functions are firstly evaluated for three different configurations of sphere and ellipse-type dome structures considering the incremental step number of nonlinear structural analysis. Then, the dominant design constraints are determined according to the violation of three design constraints named displacement, MRDC and JRDC. The primary results obtained are summarized as:

- Whereas the violation of MRDC begins and ends in the earlier incremental step numbers of nonlinear structural analysis, the number of incremental steps becomes to be higher in the violation of JRDC. Furthermore, it is also shown that the values of objective functions considering only cases of JRDC may become to be higher with respect to MRDC. Therefore, the cases of JRDC in the design of SDS has a big importance as much as MRDC's.
- It is shown that an increase in the entire weight of SDS, which implies the use of larger size of ready hot-rolled steel profiles leads to an elevation in its load-carrying capacity. Furthermore, the inclusion of diagonal members into the construction of SDS provides a higher load-carrying capacity for SDS with ellipse-shaped form than the other proposed dome configurations. Particularly, a differentiation in the size of longitudinally arched members of SDS

causes to decrease in their load-carrying capacities.

- Constructing the ellipse-shaped SDS by use of diagonal members has a big contribution to gain a higher ductility capacity.
- The higher ductility capacity of steel structures can become a big problem for the serviceability of steel structures. It is demonstrated that this dilemma existed between two issues, ductility and serviceability is easily solved thereby performing a trade-off analysis for the optimal designs according to the preference of decision-maker.
- It is displayed that the most dominant design concepts considering the violation of MRDC and JRDC becomes to be concerned with buckling, axial stress, combination of axial and bending, and yielding.
- An increase in the horizontal and longitudinal division numbers leads to a decrease in the unity values corresponding to the cases of MRDC and JRDC. Furthermore, the lack of diagonal members causes to an increase in the sensitivity of design criteria named "elastic buckling" as a case of MRDC and "combined axial and bending" and "a special control for existence of chord brace" as the cases of JRDC
- It is also displayed that an increase in the division numbers for the generation of horizontal and vertical members achieves to decrease the unity values corresponding to the cases of MRDC and JRDC

Consequently, the proposed design optimization approach is suggested for the optimal design of SDS.

References

- [1] Nowak, A. S., Collins, K. R. "Reliability of Structures", 2nd ed., CRC Press, Boca Raton, Florida, United States, 2012.
- [2] Zaeimi, M., Ghoddosian, A. "Structural Reliability Assessment Based on the Improved Constrained Differential Evolution Algorithm", *Periodica Polytechnica Civil Engineering*, 62(2), pp. 494–507, 2018. <https://doi.org/10.3311/PPci.11537>
- [3] Okasha, N. M. "Proposed Algorithms for an Efficient System Reliability-Based Design Optimization of Truss Structures", *Journal of Computing in Civil Engineering*, 30(5), 2016.
- [4] Kaveh, A., Massoudi, M. S., Bagha, M. G. "Structural Reliability Analysis Using Charged System Search Algorithm", *Iranian Journal of Science and Technology - Transactions of Civil Engineering*, 38(C2), pp. 439–448, 2014. <https://doi.org/10.22099/IJSTC.2014.2420>
- [5] Fu, F. "Structural Analysis and Design to Prevent Disproportionate Collapse", 1st ed., CRC Press, Boca Raton, Florida, USA, 2016. <https://doi.org/10.1201/b19662>
- [6] Fu, F. "Advanced Modeling Techniques in Structural Design", 1st ed., Wiley-Blackwell Press, Oxford, United Kingdom, 2015.
- [7] Izzuddin, B. A., Vlassis, A. G., Elghazouli, A. Y., Nethercot, D. A. "Progressive collapse of multi-storey buildings due to sudden column loss - Part I: Simplified assessment framework", *Engineering Structures*, 30(5), pp. 1308–1318, 2008. <https://doi.org/10.1016/j.engstruct.2007.07.011>
- [8] Marjanishvili, S., Agnew, E. "Comparison of various procedures for progressive collapse analysis", *Journal of Performance of Constructed Facilities*, 20(4), pp. 365–374, 2006. [https://doi.org/10.1061/\(ASCE\)0887-3828\(2006\)20:4\(365\)](https://doi.org/10.1061/(ASCE)0887-3828(2006)20:4(365))
- [9] Hosseini, S. M., Amiri, G. G. "Successive collapse potential of eccentric braced frames in comparison with buckling-restrained braces in eccentric configurations", *International Journal of Steel Structures*, 17(2), pp. 481–489, 2017. <https://doi.org/10.1007/s13296-017-6008-6>
- [10] Tavakoli, H. R., Kiakojouri, F. "Numerical study of progressive collapse in framed structures: A new approach for dynamic column removal", *International Journal of Engineering-Transactions A: Basics*, 26(7), pp. 685–692, 2013. <https://doi.org/10.5829/idosi.ije.2013.26.07a.02>

- [11] Byfield, M., Mudalige, W., Morison, C., Stoddart, E. "A review of progressive collapse research and regulations", *Structures and Buildings*, 167(8), pp. 447–456, 2014.
<https://doi.org/10.1680/stbu.12.00023>
- [12] Agrawal, A., Varma, A. H. "Fire induced progressive collapse of steel building structures: The role of interior gravity columns", *Engineering Structures*, 58, pp. 129–140, 2014.
<https://doi.org/10.1016/j.engstruct.2013.09.020>
- [13] McConnell, J. R., Brown, H. "Evaluation of progressive collapse alternate load path analyses in designing for blast resistance of steel columns", *Engineering Structures*, 33(10), pp. 2899–2909, 2011.
<https://doi.org/10.1016/j.engstruct.2011.06.014>
- [14] Kang, H., Kim, J. "Progressive Collapse of Steel Moment Frames Subjected to Vehicle Impact", *Journal of Performance of Constructed Facilities*, 29(6), pp. 1943–1956, 2014.
- [15] Agrawal, A., Kawaguchi, A., Chen, Z. "Deterioration Rates of Typical Bridge Elements in New York", *Journal of Bridge Engineering*, 15(4), pp. 419–429, 2010.
[https://doi.org/10.1061/\(ASCE\)BE.1943-5592.0000123](https://doi.org/10.1061/(ASCE)BE.1943-5592.0000123)
- [16] Gerasimidis, S., Deodatis, G., Kontoroupi, T., Ettouney, M. "Loss-of-stability induced progressive collapse modes in 3D steel moment frames", *Structure and Infrastructure Engineering*, 11(3), pp. 334–344, 2015.
<https://doi.org/10.1080/15732479.2014.885063>
- [17] Gao, S., Guo, L., Fu, F., Zhang, S. "Capacity of semi-rigid composite joints in accommodating column loss", *Journal of Constructional Steel Research*, 139, pp. 288–301, 2017.
<https://doi.org/10.1016/j.jcsr.2017.09.029>
- [18] Guo, L., Gao, S., Fu, F. "Structural performance of semi-rigid composite frame under column loss", *Engineering Structures*, 95, pp. 112–126, 2015.
<https://doi.org/10.1016/j.engstruct.2015.03.049>
- [19] Talasliloglu, T. "Global stability-based design optimization of truss structures using multiple objectives", *Sadhana*, 38(1), pp. 37–68, 2013.
<https://doi.org/10.1007/s12046-013-0111-y>
- [20] Talasliloglu, T. "Weight minimization of tubular dome structures by a particle swarm methodology", *Kuwait Journal of Science and Engineering*, 1(1), pp. 145–180, 2013. [online] Available at: http://pubcouncil.kuniv.edu.kw/jer/files/18Jun20130337137_Weight.pdf [Accessed: 08.04.2019]
- [21] Talasliloglu, T. "Optimal Dome Design Considering Member-related design constraints", 2019. (accepted for the *Journal of Frontiers of Structural and Civil Engineering*)
- [22] Talasliloglu, T. "Multiobjective size and topology optimization of dome structures", *Structural Engineering and Mechanics*, 43(6), pp. 795–821, 2012.
<https://doi.org/10.12989/sem.2012.43.6.795>
- [23] Lamberti, L., Pappalettere, C. "Meta-heuristic Design Optimization of Skeletal Structures: A Review", *Computational Technology Reviews*, 4, pp. 1–32, 2011.
<https://doi.org/10.4203/ctr.4.1>
- [24] Yang, X.-S. "Engineering Optimization: An Introduction with Metaheuristic Applications", 1st ed., Wiley, Hoboken, New Jersey, United States, 2010.
- [25] Hasancebi, O., Erdal, F., Saka, M. P. "Optimum Design of Geodesic Steel Domes Under Code Provisions Using Meta-heuristic Techniques", *International Journal of Engineering Applied Science*, 2(2), pp. 88–103, 2010. [online] Available at: <http://dergipark.gov.tr/download/article-file/217622> [Accessed: 08.04.2019]
- [26] Talasliloglu, T. "Multi-objective Design Optimization of Geometrically Nonlinear Truss Structures", *Kuwait Journal of Science and Engineering*, 39(2), pp. 47–77, 2012.
- [27] Kalyanmoy, D., Amrit, P., Sameer, A., Meyarivan, T. "A fast elitist multiobjective genetic algorithm: NSGA-II", *IEEE Transactions on Evolutionary Computation*, 6(2), pp. 182–197, 2002.
<https://doi.org/10.1109/4235.996017>
- [28] Beume, N., Naujoks, B., Emmerich, M. "SMS-EMOA: Multi-objective selection based on dominated hypervolume", *European Journal of Operational Research*, 181(3), pp. 1653–1669, 2007.
<https://doi.org/10.1016/j.ejor.2006.08.008>
- [29] Zhang, Q., Li, H. "MOEA/D: A multiobjective Evolutionary Algorithm Based on Decomposition", *IEEE Transactions on Evolutionary Computation*, 11(6), pp. 712–731, 2007.
<https://doi.org/10.1109/TEVC.2007.892759>
- [30] Corne, D. W., Jerram, N. R., Knowles, J. D., Oates, M. J. "PESA-II: Region-based Selection in Evolutionary Multiobjective Optimization", In: *Proceedings of the Genetic and Evolutionary Computation Conference, GECCO 2001, San Francisco, California, United States, 2001*, pp. 283–290. [online] Available at: <http://citeseerx.ist.psu.edu/viewdoc/download?doi=10.1.1.10.2.194&rep=rep1&type=pdf> [Accessed: 08.04.2019]
- [31] Zitzler, E., Laumanns, M., Thiele, L. "SPEA2: Improving the Strength Pareto Evolutionary Algorithm for Multi-objective Optimization", In: *Proceedings of the Fifth Conference on Evolutionary Methods for Design, Optimization and Control with Applications to Industrial Problems, EUROGEN 2001, Athens, Greece, 2001*, pp. 95–100. [online] Available at: <http://www.gbv.de/dms/tib-ub-hannover/37304500X.pdf> [Accessed: 08.04.2019]
- [32] Deb, K., Mohan, M., Mishra, S. "Towards a Quick Computation of Well-Spread Pareto-Optimal Solutions", In: *Proceedings of the International Conference on Evolutionary Multi-Criterion Optimization, EMO 2003, Faro, Portugal, 2003*, pp. 222–236.
https://doi.org/10.1007/3-540-36970-8_16
- [33] Kaveh, A., Raissi Dehkordi, M. "RBF and BP Neural Networks for the Analysis and Design of Domes", *International Journal of Space Structures*, 18(3), pp. 181–194, 2003.
<https://doi.org/10.1260/026635103322437463>
- [34] Kaveh, A., Talatahari, S. "Optimal design of Schwedler and ribbed domes via hybrid Big Bang - Big Crunch algorithm", *Journal of Constructional Steel Research*, 66(3), pp. 412–419, 2010.
<https://doi.org/10.1016/j.jcsr.2009.10.013>
- [35] Kaveh, A., Talatahari, S. "Optimal Design of Single Layer Domes Using Meta-Heuristic Algorithms: a Comparative Study", *International Journal of Space Structures*, 25(4), pp. 217–227, 2010.
<https://doi.org/10.1260/0266-3511.25.4.217>
- [36] Kaveh, A., Talatahari, S. "Geometry and topology optimization of geodesic domes using charged system search", *Structural and Multidisciplinary Optimization*, 43(2), pp. 215–229, 2011.
<https://doi.org/10.1007/s00158-010-0566-y>

- [37] Kaveh, A., Rezaie, M. "Optimum topology design of geometrically nonlinear suspended domes using ECBO", *Structural Engineering and Mechanics*, 56(4), pp. 667–694, 2015.
<https://doi.org/10.12989/sem.2015.56.4.667>
- [38] Kaveh, A., Rezaie, M. "Topology and geometry optimization of different types of domes using ECBO", *Advances in Computational Design*, 1(1), pp. 1–25, 2016.
<https://doi.org/10.12989/acd.2016.1.1.001>
- [39] Kaveh, A., Rezaie, M. "Topology and geometry optimization of single-layer domes utilizing colliding bodies optimization", *Scientia Iranica*, 23(2), pp. 535–547, 2016.
<https://doi.org/10.24200/SCI.2016.2137>
- [40] Kaveh, A., Ilchi Ghazaan, M. "Optimal design of dome truss structures with dynamic frequency constraints", *Structural and Multidisciplinary Optimization*, 53(3), pp. 605–621, 2016.
<https://doi.org/10.1007/s00158-015-1357-2>
- [41] Kaveh, A., Ilchi Ghazaan, M. "A new hybrid meta-heuristic algorithm for optimal design of large-scale dome structures", *Engineering Optimization*, 50(2), pp. 235–252, 2018.
<https://doi.org/10.1080/0305215X.2017.1313250>
- [42] Kaveh, A., Rezaei, M., Shiravand, M. R. "Optimal design of nonlinear large-scale suspended domes using cascade optimization", *International Journal of Space Structures*, 33(1), pp. 3–18, 2018.
<https://doi.org/10.1177/0266351117736649>
- [43] Kaveh, A., Rezaei, M. "Optimal Design of Double-Layer Domes Considering Different Mechanical Systems via ECBO", *Iranian Journal of Science and Technology, Transactions of Civil Engineering*, 42(4), pp. 333–344, 2018.
<https://doi.org/10.1007/s40996-018-0123-2>
- [44] Kaveh, A., Javadi, S. M. "Chaos-based firefly algorithms for optimization of cyclically large-size braced steel domes with multiple frequency constraints", *Computers and Structures*, 214, pp. 28–39, 2019.
<https://doi.org/10.1016/j.compstruc.2019.01.006>